Hindawi
Advances in Civil Engineering
Volume 2022, Article ID 8632920, 15 pages
https://doi.org/10.1155/2022/8632920

Research Article

Effect of the Wall-Back Inclination Angle on the Inertial Loading Distribution along Gravity-Retaining Walls: An Experimental Study on the Shaking Table Test

Shuzhi Ma,[1] **Hongbiao Jia**,[1] **and Xiaolang Liu**[2]

[1]*Engineering Faculty, China University of Geosciences (Wuhan), Wuhan 430074, China*
[2]*Bijie Transportation Development Service Center, Bijie 551700, China*

Correspondence should be addressed to Shuzhi Ma; mashuzhi@cug.edu.cn

Received 21 July 2022; Revised 2 December 2022; Accepted 12 December 2022; Published 23 December 2022

Academic Editor: Castorina S. Vieira

The gravity-retaining wall is a common retaining structure in geotechnical engineering. The inertial load acting on the retaining wall itself (the horizontal seismic action) under earthquake conditions is one of the major loadings to be elaborately considered for the design of gravity-retaining walls. The horizontal seismic action of the retaining walls under seismic loading is dominated by the combination of the mass distribution of the wall body and the acceleration distribution along wall height. The mass distribution can be calculated by the wall geometry and density of the wall body. By contrast, due to the whipping effect, horizontal seismic acceleration along wall height often shows obvious amplification in relation to ground acceleration. Such a distribution of acceleration amplification is of great importance to comprehend the safe design of retaining walls. Nonvertical retaining walls, such as inclined and reclined retaining walls, are often used in practical engineering, and their dynamic responses under seismic actions will be different from those of vertical walls. This paper focused on the examination of the influence of the wall-back inclination angle of retaining walls on the dynamic acceleration distribution along wall height due to seismic actions. Dynamic responses of vertical, inclined, and reclined gravity retaining walls under various earthquake loads were tested on a shaking table system. Seismic acceleration time-history curves were recorded under different seismic waves and intensities. The influence of the wall-back inclination angle of retaining walls on the seismic effect was thus analyzed. The tested results showed that the wall-back inclination angle of retaining walls has a significant influence on the seismic dynamic response. The amplification coefficients of peak acceleration of the gravity retaining wall follow the order of the reclined type > the vertical type > the inclined type. Based on the experimental results, the amplification coefficient of peak acceleration was statistically analyzed under the commonly used risk level in engineering seismic design. A formula for the calculation of the horizontal earthquake action distribution coefficient along wall height was proposed involving the effect of the wall-back inclination angle, which might improve the existing calculation method of retaining wall design. The results of this work would guide the earthquake resistance dynamic design of retaining walls.

1. Introduction

The gravity-retaining wall is a common retaining structure in geotechnical engineering. It is usually built on the ground and extends upwardly to the top end, thereby forming a barrier obstructing the movement of soil behind. The seismic effect can significantly deteriorate the stability of the retaining wall, even rendering the failure (collapse) of the wall under strong seismic conditions. Due to the whipping effect, the seismic action can transform and get increasingly intensified along the wall height from the heel. Such an amplification effect is affected not only by the seismic load but also by the retaining wall itself, the backfill behind the wall, site conditions, etc. Due to the diversity of these factors, it remains a challenge for precise design and prediction for the seismic response of the retaining wall [1, 2]. The distribution of seismic inertia action along the wall height is complex. In the analysis and calculation of the seismic strength and stability of the retaining wall, the seismic inertia action at different heights of the retaining wall is one critical

content. As such, it is of particular significance to comprehend the dynamic response of retaining walls to earthquakes and develop a reasonable distribution relation to responsive horizontal seismic action along the wall height for more appropriate seismic design of retaining walls [3–5].

Inertial loading sustained by the retaining wall originates from its intrinsic weight of the wall and acceleration responding to seismic action. The amplification effect of horizontal seismic action at a certain height of the wall is characterized as the relative seismic acceleration at that height to the one at the wall heel. To characterize the amplification effect of the inertial loading on the wall derived from seismic action, a term denoted as the distribution coefficient of horizontal seismic action along the wall height ψ_i is usually used, which is defined as the ratio of seismic peak acceleration at a specific wall height (e.g., section i) to the retaining wall axis and the peak ground acceleration value (PGA). The research regarding the response of retaining walls to seismic effects mainly focused on the variation of ψ_i along wall height.

A previous study by the Sichuan Institute of Building Sciences in the 1980s carried out the shaking table test on a 6 m high retaining wall; ψ_i at the wall top was in the range of 1.37~1.93 [6]. The result of this study and other dynamic test results of retaining walls and earth dams constituted the seismic design as per the Chinese Specification of Seismic Design for Highway Engineering (JTJ 004-89) [6]. It adopts a two-height rule, which classifies walls into 2 groups: walls lower than 12 m and walls higher than 12 m. When walls are lower than 12 m, horizontal acceleration is regarded as having no amplification along wall height, i.e., $\psi_i = 1$; when walls are higher than 12 m, ψ_i starts to increase linearly from 1 at the wall heel to 2 at the wall top. Note that such a design strategy appears somewhat rough or oversimplified, as ψ_i is regarded as invariable uniformity lower than 12 m.

A large number of earthquake damage phenomena show that the seismic response varies significantly with wall height, and the distribution of horizontal seismic response acceleration along height is rather complex. Chen [7], Zhou [8], Xu [9], and Li et al. [10] have investigated the seismic acceleration response of gravity retaining walls at different heights via numerical simulations. Studies show that the smaller amplification effect below middle height is about 0.5~0.7 times the height of the retaining wall, while above middle height, the amplification effect of seismic acceleration increases evidently with wall height and reaches the highest value of around 1.1~2.0 times the height of the bottom [7–10]. A research group, with the participation of Tongji University, Institute of Engineering Mechanics of China Earthquake Administration, etc., found that acceleration amplification shows a relatively less increment below 1/2~2/3 of the total height of the retaining wall, whereas beyond which it starts to increase more obviously, and ψ_i reaches the maximum value of 1.2~2.0 at the wall top [11]. A general concept was recognized that higher retaining walls are more prone to seismic damage at their upper parts.

Based on the relevant research results and engineering experience, taking risk statistics into consideration, a formula for calculating ψ_i is determined and adopted for modified seismic design use of retaining walls as per the Chinese Specification of Seismic Design for Highway Engineering (JTG B02-2013) [11]. In contrast to the previous version, this new formula takes two respective linear relationships for determining ψ_i, with a relative height of 0.6 H as turning height. Such a treatment overcomes the uniform value of ψ_i of 1 (no amplification effect) for lower height wall (<12 m) and the intermittent issue of ψ_i at 12 m.

Herein, it is worth pointing out that retaining walls can be roughly classified into three categories, reclined, vertical, and inclined back walls based on the wall-back slope in relation to the vertical direction. Although the above-mentioned research mainly focused on vertical retaining walls [6–11], the influence of the back inclination of the retaining wall is rarely considered. Actually, nonvertical retaining walls, such as inclined and reclined retaining walls, are often used in practical engineering, and their wall-back slopes may be different. Retaining walls with different back slopes may also have different earthquake influences on their dynamic responses. Yet the study of retaining walls rarely involves the influence of retaining wall-back inclination on the acceleration amplification factor.

The shaking table test is an important method for studying the dynamic response of retaining walls because it can simulate the process of earthquake action. The shaking table test of retaining walls began in the 1970s [12, 13]. In recent years, shaking table model experiments have been widely used to study the dynamic response of gravity-retaining walls [8, 14–19] and other types of retaining walls (such as cantilever-retaining walls [20], geosynthetic-reinforced soil-retaining walls [21, 22], soil bag-retaining walls [23], geogrid-reinforced retaining walls [24], and reinforced retaining walls by anchored piles [1]). However, the shaking table test of gravity-retaining walls is mostly about dynamic lateral earth pressure or stability of retaining walls, and there are few studies on the ψ_i of gravity-retaining walls. In spite of this, the experimental schemes and valuable results of these studies guided the scheme design and data analysis of the shaking table test of the retaining wall in this paper.

As such, using the shaking table simulation test, this work focused on the comparative study on the dynamic response of three characteristic types of gravity-retaining walls, inclined, reclined, and vertical retaining walls, with respect to seismic actions. The influence of retaining wall types (the wall-back slope) on the distribution of seismic acceleration along wall height was analyzed. A calculation formula for the distribution coefficient of horizontal seismic action along the wall height comprising the influence of wall-back slopes was proposed. This work would help improve the rationality of the seismic design of retaining walls.

2. Shaking Table Test on Retaining Walls

2.1. Retaining Wall Model. The shaking table experiments were carried out on a custom-designedhorizontal-vertical two-way hydraulic shaking table system at the China University of Geosciences (Wuhan). The platform size was 1 m × 2 m, the maximum load capacity was 250 kg, and the

maximum driving acceleration was 20 m/s^2 (2.0 g). Analogy models with a reduced scale were used to mimic the actual retaining walls under seismic conditions in the model experiment. As restricted by the bearing capacity of the shaking table system (250 kg) and the back in the model experiment, a model test box with designated 3D dimension ratios was predetermined [14–25]; the dimensions of the model test box were set to 1 m × 0.4 m × 0.5 m. The height of the model-retaining wall H was designated at 0.4 m, while the wall bottom was set horizontally. Three typical retaining walls were used, i.e., reclined, vertical, and inclined walls, respectively. The slopes of the wall-back face of such retaining walls in relation to the vertical direction were designated at −20°, 0°, and 20°, representing reclined, vertical, and inclined retaining walls, respectively. Such a slope range covers most of the inclination angles of retaining walls [2].

To circumvent the experimental deviation caused by different weights of the wall models on the experimental results, all three types of walls adopted a unified volume to ensure essentially consistent weight. The cross-sections of the three types of wall models are shown in Figure 1. All the wall models were of the same thickness of 0.5 m.

2.2. Model Similarity Relationship. As this work adopted a reduced-scale simulation test, a rational similarity between the real situation and the model test is important for the accurate reflection of the actual shaking effect. In this work, the height of the prototype retaining wall H_0 was set at 12.5 m, as this height is a typical one that is close to the turning height, differentiating between low and high walls, and within the range of the high wall for ψ_i determination [11]. We employed the similarity principle of the model experiment [8, 14] to determine the values of physical quantities of the retaining wall model. As described in Section 2.1, the height of the retaining wall model is set at 0.4 m, based on the size of the model box and the input/output frequency range of the shaking table system, so the similarity coefficient of length $C_H = H_0/H = 12.5/0.4 = 31.25$. The experiments were carried out in a 1 g gravitational field, and the similarity coefficient of density C_ρ and acceleration C_a were both taken as 1 [26–30]. The wall height H, density of backfill ρ, and acceleration were selected as control parameters. The deduced similarity coefficients of simulated physical quantities are tabulated in Table 1. The similar coefficient of time (C_t) was used as an input control factor for performing simulations of acceleration time histories of different seismic motions.

2.3. Preparation of Backfill Soil. According to the similarity principle and ratio in Table 1, the physical and mechanical parameters of the backfill of the shaking table test were designated, as shown in Table 2. It can be seen that the backfill soil used in the test should be of low strength. Thus, a mixture comprising various components with different mechanical properties was used. The backfill of the wall was prepared based on literature in [8, 9, 14]. Through trial preparation tests on different content ratios of various materials, the resultant backfill recipe was obtained as 1clay: 5 barite powder: 2 quartz sand: 1carbonate of lime powder: 1 talc powder by relative weight ratios. The clay was sampled from the reservoir basin of the Three Gorges Reservoir from Zigui County, China, and used after drying, grinding, and impurity removal. The properties of this mixed soil were essentially consistent with those of the majority of soils in soil mechanics

2.4. Layout of the Model Box and the Embedding of Monitors. As above mentioned, the dimensions of the model test box were 1 m × 0.4 m × 0.5 m. A concrete block (0.4 m × 0.2 m × 0.1 m) was put at the front end of the model box to hamper the horizontal displacement of the retaining wall during the test. 3 cm thick foam was laid between the back wall of the model box and the backfill to absorb wave energy and reduce the boundary effect [1, 31]. The whole model extended horizontally along the strike direction of the retaining wall. To monitor the acceleration at different heights of the wall body during the test, 6 accelerometers were fixed at different relative heights (h_i = 0H, 1/5H, 2/5H, 3/5H, 4/5H, and 1H, respectively) on the wall-back axis of the model. In addition, another accelerometer (A0) was arranged on the model box to estimate the response of the shaking table system during the experiment. As an example, the accelerometer layout for the case of the reclined wall is illustratively shown in Figure 2.

The back space of the model wall was filled with as-prepared soil and subject to layer-by-layer pressing until the desired density (≥90% of the required compaction volume) was achieved. When all layers were filled, backfill was compacted under vibration with low intensity until the density reached the required model backfill density (as shown in Table 2). The actual experimental model after filling is shown in Figure 3.

2.5. Dynamic Loading Scheme Design. To investigate the influence of different seismic waves and intensities on the dynamic response of the retaining wall, three typical seismic waveforms were used in the test: the Kobe wave, Wenchuan wave, and EL Centro wave. The seismic waves applied for loading were obtained through wave filtering, baseline correction, and removing the weak seismic part of small amplitude in the later earthquake stage from the three original seismic waves [14]. The peak acceleration of each loaded wave was set at 0.1 g, 0.2 g, 0.4 g, and 0.6 g, respectively, to simulate the seismic intensity of peak ground acceleration (PGA) of VII, VIII, IX, and >IX levels of the earthquake.

Prior to seismic wave loading, the test system was loaded with a white noise of 0.3 m/s^2 to observe the response of the shaking table and the model system to ensure normal working conditions. According to Table 1, the input wave time compression ratio was adjusted to 5.6 to obtain similar dynamic response characteristics as those of the prototype retaining wall with a height of 12.5 m. Upon wave loading, the resultant response acceleration waves at each monitoring point on the back of retaining walls were recorded. For the

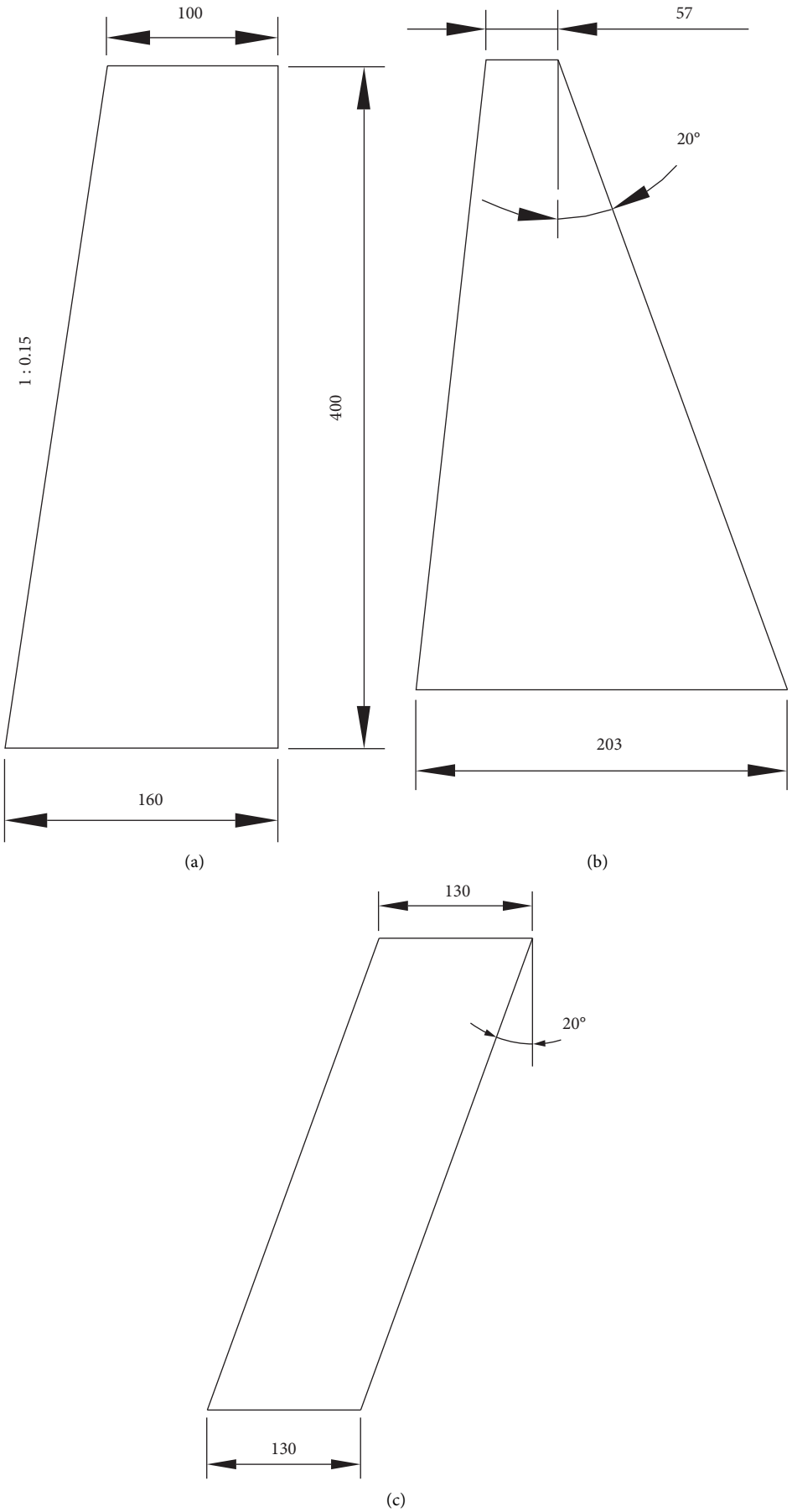

Figure 1: Wall model size of retaining walls (unit: mm). (a) Vertical walls. (b) Inclined walls. (c) Reclined walls.

Table 1: Similarity relationship of the main physical quantities of the retaining wall model.

Items	Acceleration a	Backfill density ρ	Height H	Time t	Backfill cohesion c	Backfill internal friction angle φ
Similarity relationship	C_a	C_ρ	C_H	$C_t = C_a^{-1/2}C_H^{1/2}$	$C_c = C_aC_\rho C_H$	C_φ
Similarity coefficient	1	1	31.25	5.6	31.25	1
Remark	Control factor	Control factor	Control factor	Input control		

Table 2: Main physical and mechanical parameters of prototype soil and model materials.

Items	Height H (m)	Density ρ (g·cm^{-3})	Cohesion c (kPa)	Internal friction angle φ (°)	Water content w (%)
Backfill of prototype walls	12.5	2.1	43.9	31	10
Backfill of wall models	0.4	2.1	1.40	31	10

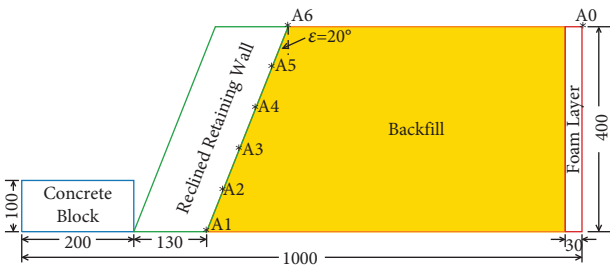

Figure 2: Accelerometer layout and embedding of monitors (unit: mm).

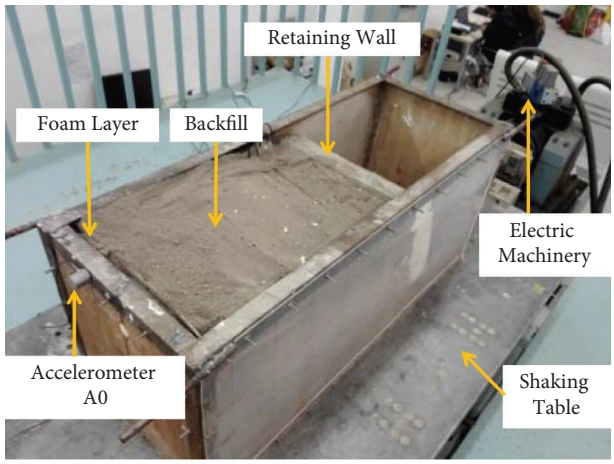

Figure 3: Experimental model.

three types of retaining walls, the shaking table tests were carried out under three vibration waveforms and four peak accelerations, respectively; i.e., the monitoring data under 12 working conditions were obtained for each type of retaining wall, with 36 groups of data for the three types of retaining walls in total.

3. Results and Discussion

3.1. Rationality of Tested Vibration Waves. As an instance, a real-time dynamic response of the retaining wall to the wave input in the shaking table test is the premise for the accurate tested results and rational analysis. To make sure whether the test system truly reflected the dynamic response, we compared the responsive acceleration history waves measured at different heights with the input ones. Figure 4 presents the waveforms of the Kobe wave, Wenchuan wave, and EL Centro wave (with PGA = 0.6 g) after baseline correction in the initial 30 seconds. This input vibration wave used in the shaking table test was obtained by time compression and amplitude transformation from the original wave. Figure 5 shows the recorded acceleration history curves at monitoring points A1 (at the heel of the wall) and A6 (at the top of the wall) when the reclined retaining wall is loaded with three waves, as shown in Figure 4. Note that A1 is the closest to the wave input position among the installed monitors; its vibration should show the best consistency to the wave input. Meanwhile, the dynamic response of A6 should be strongest as it is positioned at the top of the wall. They were thus selected to examine the uniformity of responsive waves with input vibrations.

By comparing the acceleration history curves of monitoring points A1 and A6, it can be seen that the vibration of A1 and A6 is essentially synchronous and that the occurrence of major amplitude peaks is consistent with each other. The acceleration history curves of A1 and A6 are also well synchronized with those of the input wave. Besides, the peak acceleration of A1 is around 6.0 m/s^2, essentially identical to the peak acceleration (0.6 g) of the input wave. Such a consistency either in the peak position or in intensity confirms a real-time shaking table response during the test and a good wave absorption ability of the foam inserted between the model box and backfill. In addition, Figure 5 also exhibits that the acceleration at the top of the wall (A6) is larger than that at the heel of the wall (A1), especially at points of greater amplitude. Maximum acceleration reaches 10.1 m/s^2, about 1.68 times of A1. This is due to the fact that A6 is located at the top of the wall. The amplification effect of seismic acceleration leads to stronger intensity of response to wall height. Such an observation agrees with the literature results [8, 10], thereby indicating that the test results are reasonable and reliable. Likewise, other tested dynamic responses of retaining walls show similar uniformity to input waves, and they were not shown here for clarity.

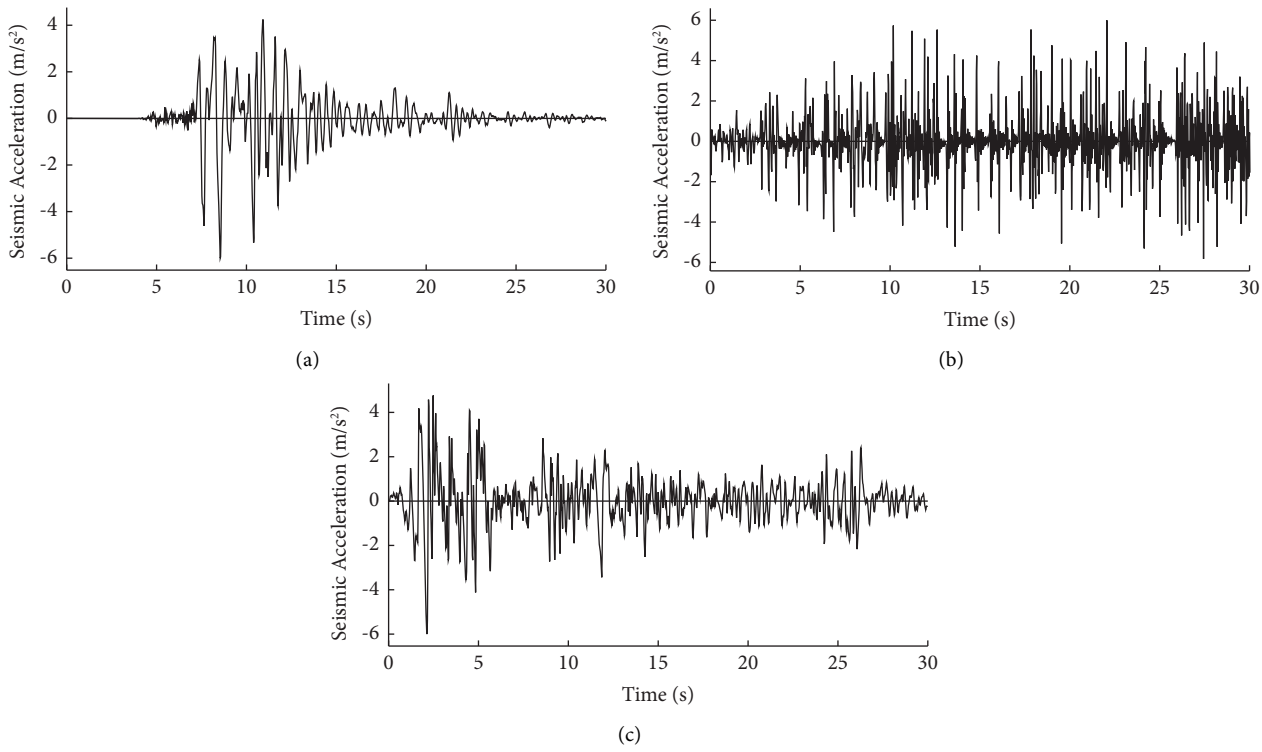

Figure 4: Three waveforms loaded on the shaking table (0.6 g). (a) Kobe wave. (b) Wenchuan wave. (c) EL Centro wave.

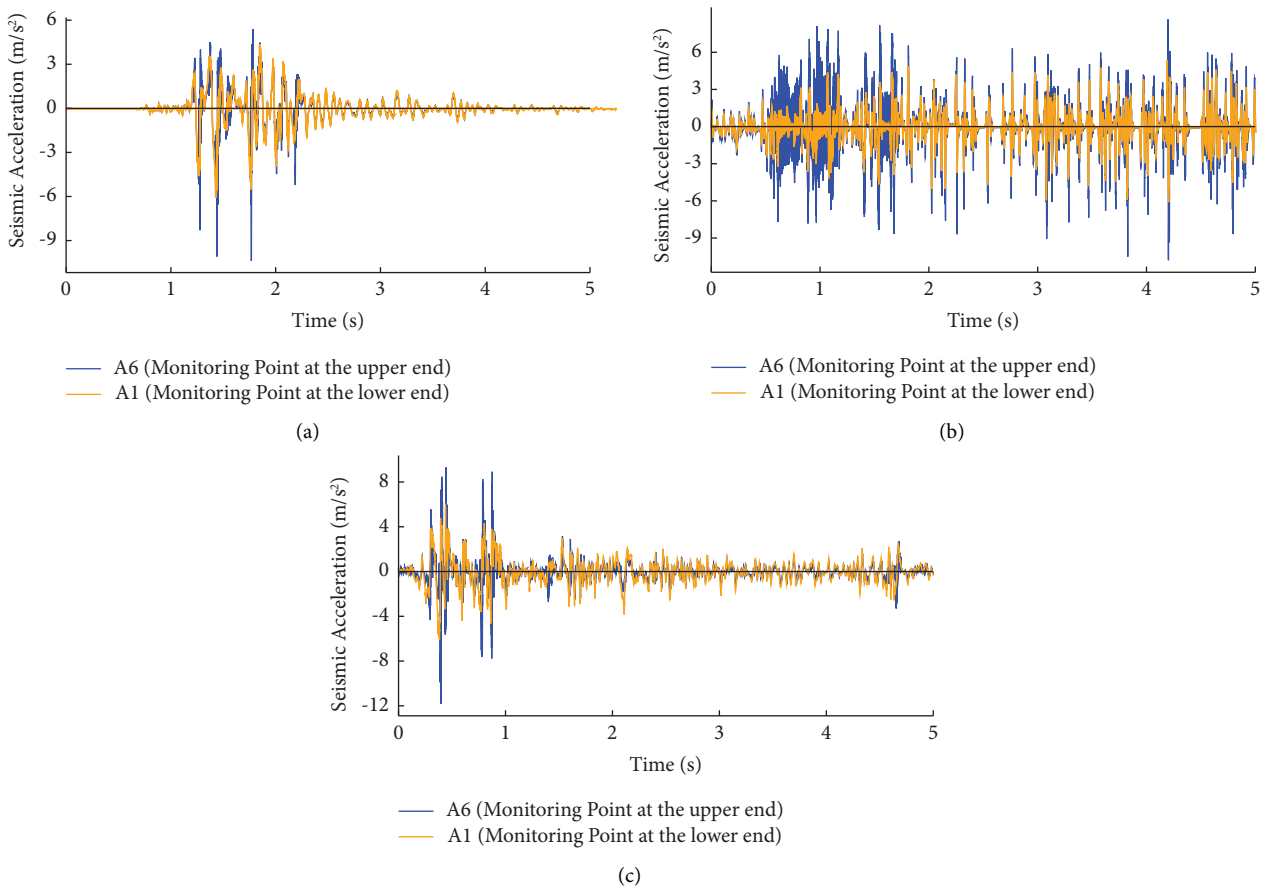

Figure 5: A1 and A6 acceleration history curves of reclining walls ($\varepsilon = -20^{\circ}$, 0.6 g). (a) Kobe wave. (b) Wenchuan wave. (c) EL Centro wave.

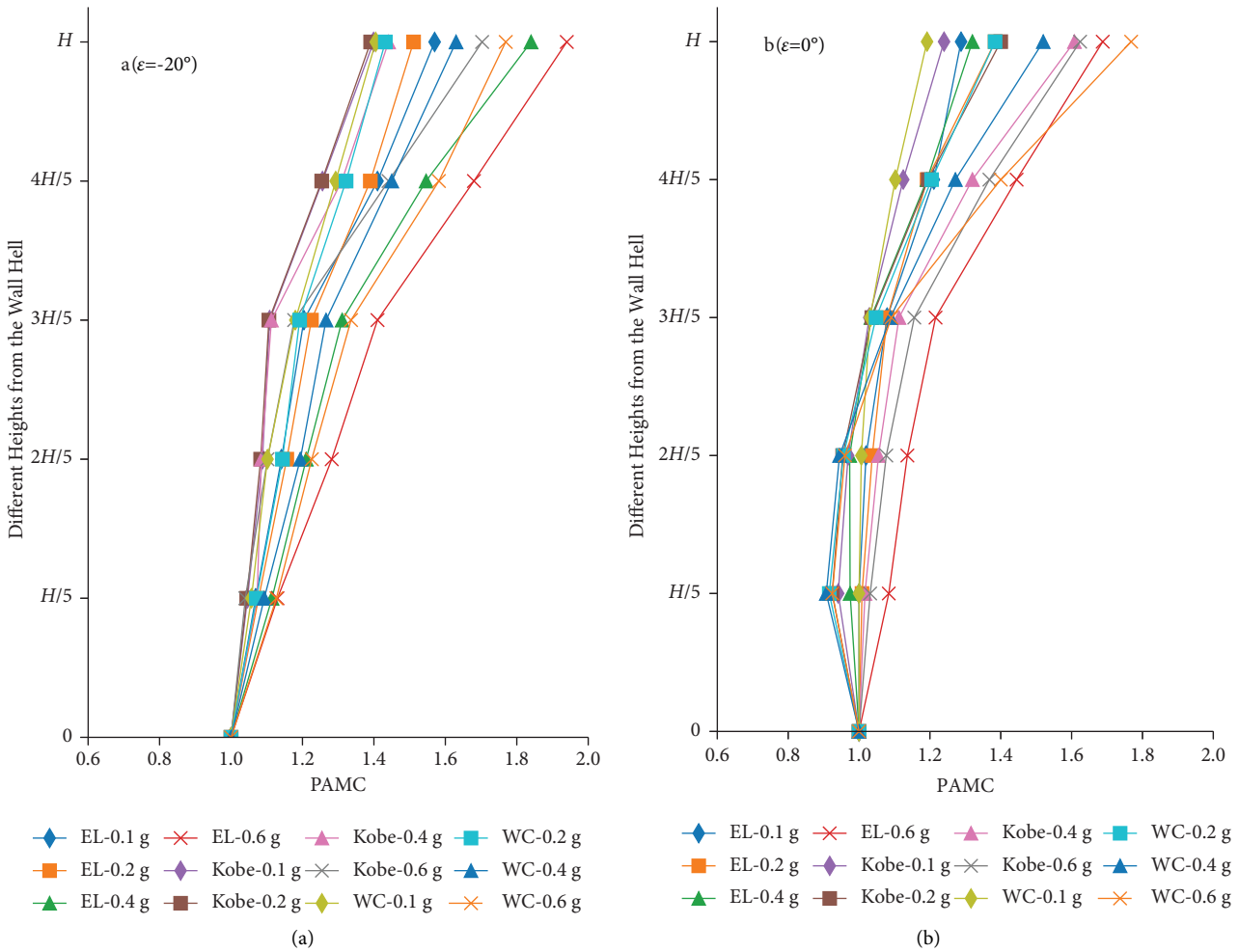

Figure 6: Continued.

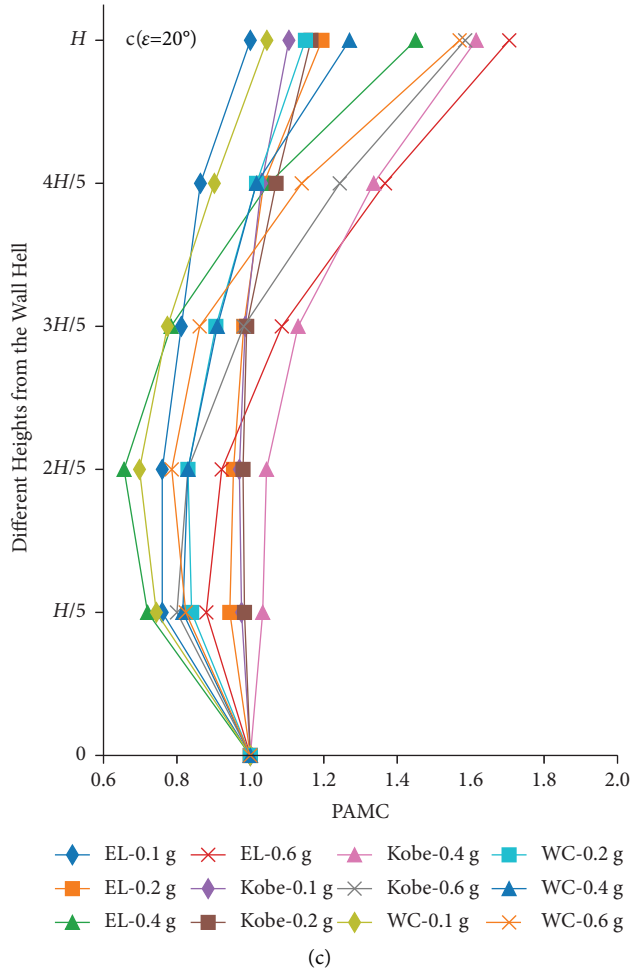

Figure 6: PAMC along wall height. (a) Reclined wall. (b) Vertical wall. (c) Inclined wall.

3.2. Influence of the Wall-Back Face Slope on the Seismic Response. The peak values of acceleration at different wall heights represent the intensity of the dynamic response thereof. To clarify the variance of the dynamic response along the wall height, the relative ratio of the acceleration peak at a specific height to the one at the wall foot, i.e., the peak acceleration magnification coefficient (PAMC), was used to depict the distribution of the dynamic response along the wall. In order to analyze the influence of wall-back inclination, the PAMC of different types of retaining walls under all input waves with different intensities and waveforms was integrated, as shown in Figure 6. For a clearer comparison, we also averaged the PAMC values under the same wave intensities and presented those versus relative wall height in Figure 7.

From Figures 6 and 7, it can be seen that, for all wall-back slopes, PAMCs reach the highest value at the top of the wall, indicating the amplification phenomena of the seismic whipping effect. However, the PAMC values and variance in relation to wall height differ significantly with wall-back inclinations. For the reclined wall, all the PAMC data show values greater than 1, indicating a steady amplification effect along the wall. By contrast, the vertical and the inclined wall exhibited PAMCs less than 1 at lower wall height. Such reduced PAMCs imply the alleviation effect relative to the input wave. Only above the specific height (0.2 H and 0.4 H for the vertical wall and the inclined wall, respectively), the PAMC starts to show an amplification effect (PAMC > 1).

On the other hand, the increasing extents of different wall-back slopes also differ greatly. It can be seen from Figure 7(a) that the PAMC of the reclined wall shows a mild increase below 0.6 H, and beyond this, PAMCs increase more evidently. For vertical walls and inclined walls, PAMCs initially reduce to less than 1 (alleviation of the input wave) and then shortly recover to 1. Above such turning height, PAMCs increase dramatically. All three walls appear to exhibit approximately similar increasing linear relationships beyond 0.6 H and reach the highest value at the top of the wall. The order of the highest PAMC is the reclined wall- > vertical wall > inclined wall, indicating the intensified dynamic response with the decreased wall-back slope. Besides, the PAMC values of vertical and reclined retaining walls are relatively concentrated at the same height, while those of inclined walls are relatively scattered, especially below 0.6 H, indicating that the amplification effect of seismic waves varies greatly for inclined retaining walls.

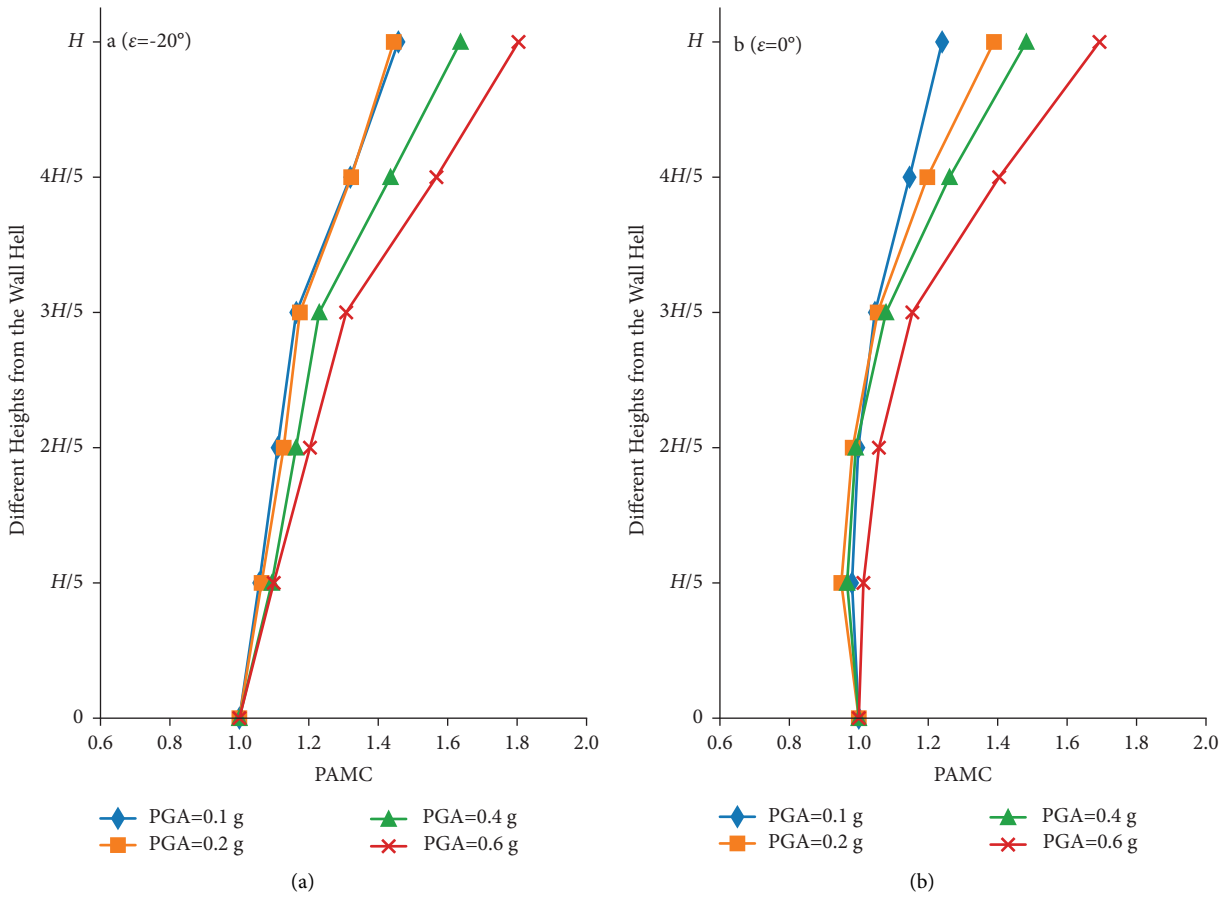

Figure 7: Continued.

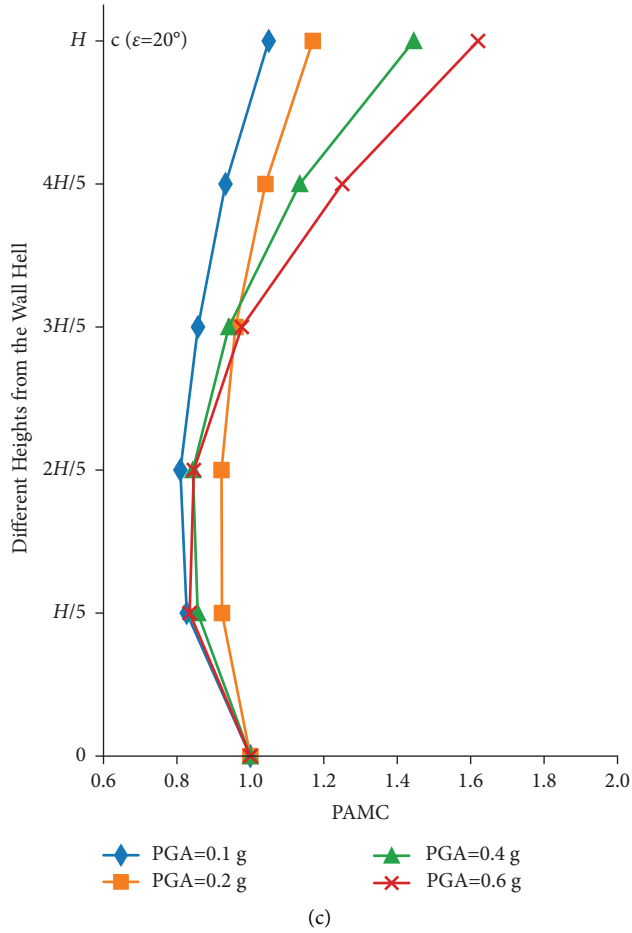

Figure 7: Average PAMC along wall height. (a) Reclined wall. (b) Vertical wall. (c) Inclined wall.

Figure 7 also shows that the amplification effect of peak seismic acceleration is affected by seismic intensity but not by seismic wave types. The higher the seismic intensity, the more significant the amplification effect, which is consistent with the research results of Ren [14]. Despite this, in order to get a clearer rule of the influence of the back inclination of the wall on the amplification effect and to express it with mathematical formulas, the influence of seismic intensity on the amplification factor was ignored, and the test results under different seismic intensities were analyzed together. At the same time, it is expected that follow-up research can obtain more perfect practical calculation formulas by considering more factors.

Nevertheless, the above observations confirm the significant effect of the wall-back slope on the distribution of the dynamic response (inertial loading) along the wall. As such, the influence of wall-back inclination should be considered for the dynamic design of retaining walls in a more reasonable manner.

3.3. Distribution Coefficient ψ_i and Its Proposed Expression. The current design of retaining walls in China mostly uses the distribution coefficient of horizontal seismic action along the wall height (ψ_i) to denote the dynamic response degree of the earthquake at a specific height of the retaining wall [6, 11]. In other words, ψ_i is the designated PAMC at height of section i used in practical geoengineering design. In fact, different dynamic loads, on-site conditions, practical retaining walls, and backfills have a respective effect on the PAMC at different wall heights (ψ_i), and these factors are naturally variable during the service duration of retaining walls. Therefore, it is necessary to carefully consider the impact of the variance of such factors on the seismic acceleration amplification effect while determining the value of ψ_i at a sufficient security level of risk statistics. Since the risk assurance level used in ψ_i design is within 90% probability [6, 8, 10, 11], which is also the risk control standard commonly used in seismic engineering design, we also adopt such a risk security level to determine the distribution coefficient of horizontal seismic action (ψ_i) along the wall height for later analysis.

To make clearer determination of the distribution coefficient of each type of retaining wall, we presented the dispersion of the tested PAMCs at different heights in a statistical box plot with default settings, as shown in Figure 8. To facilitate the correlation of ψ_i with the relative height ratio (h_i/H, h_i is the height of section i in the retaining wall) of the retaining wall, the PAMC were presented versus hi/H in Figure 8. Each type of retaining wall has 12 data at

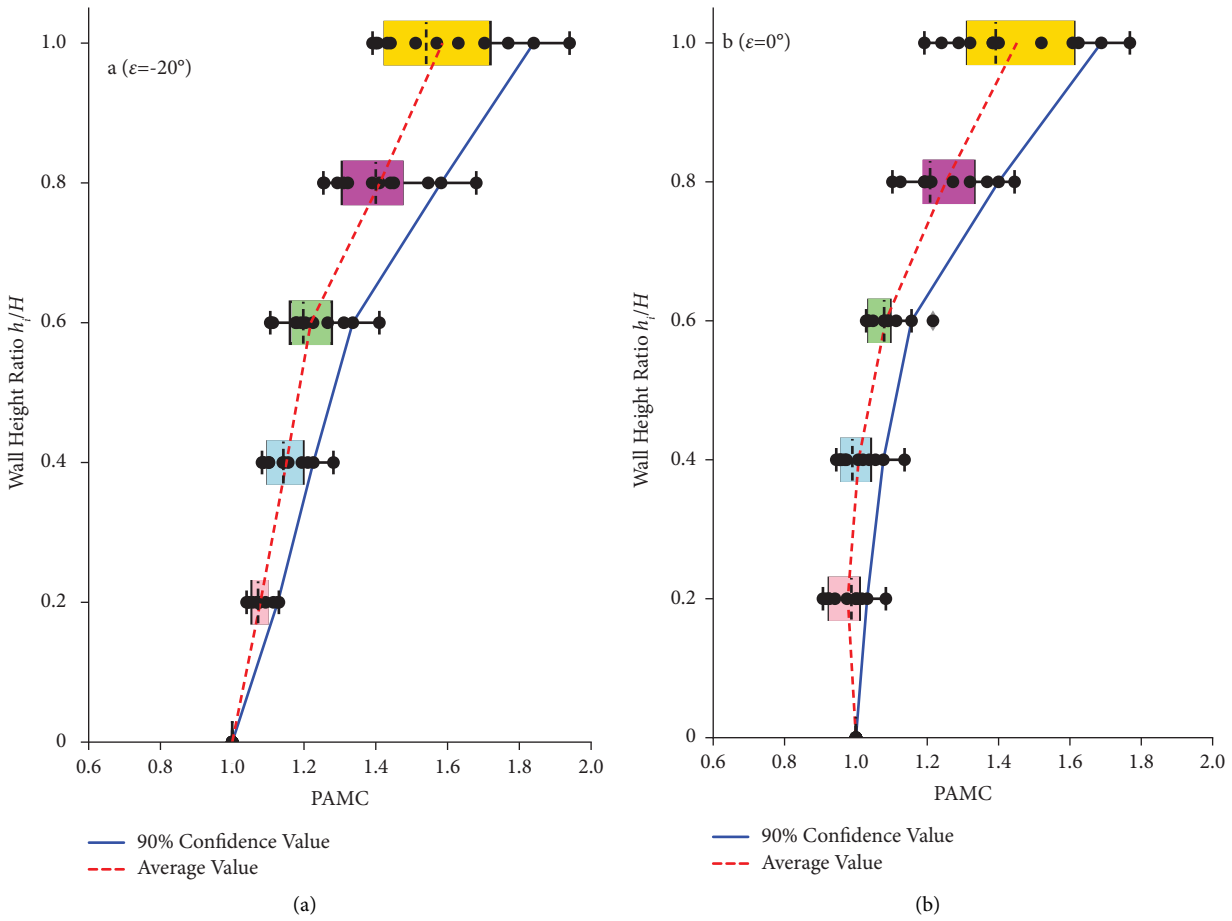

Figure 8: Continued.

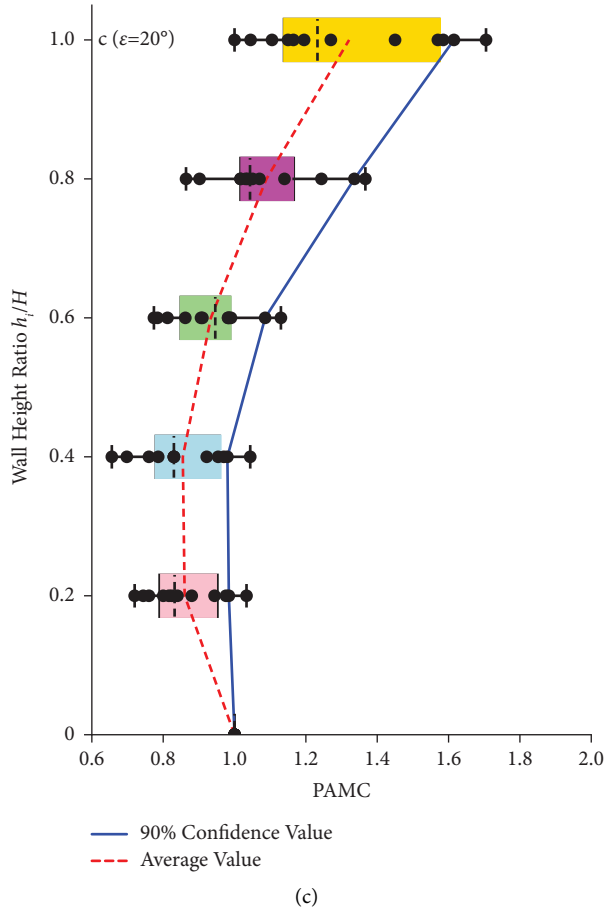

Figure 8: Analysis diagram of the acquisition method of the distribution coefficient ψ_i. (a) Reclined wall. (b) Vertical wall. (c) Inclined wall.

each monitoring point under different seismic wave types and intensities. 90th percentile values can be approximately assigned as the second largest values, which are connected by the blue line, as shown in Figure 8.

From the box diagram in Figure 8, only one abnormal data at 0.6 h_i/H for the vertical retaining wall can be observed falling outside of the statistic box. The other data points are well within the range of the upper and lower limit edge lines. The second largest value of each measuring point is positioned within the normal statistical range of the data. Therefore, it is reasonable to take the second largest value at each monitoring point as the distribution coefficient to meet the requirements of the risk level.

To explain the differences in distribution coefficients between three types of retaining walls, the connecting lines in Figure 8 are compiled into Figure 9. As it can be seen, distribution coefficients not only vary along the wall height but also depend on the types of retaining walls, i.e., different wall-back face slopes. In general, with an increase in the inclination of the wall back, the distribution coefficient decreases at the same height. The order of the distribution coefficient is reclined > vertical > inclined. In addition, it is worth noting that for all three lines, the height of 0.6 h_i/H is roughly a turning point, and after that, the wall-back face slope ε mainly affects the intercept of fitting curves, but the slopes of the curves remain essentially similar. However, below that, the fitting curves have the same intercept,but different slopes.

As discussed in Section 3.2, the degree of the seismic dynamic response of the retaining wall is significantly affected by the wall-back slope. By summarizing the above observations and discussion, we adopted different calculation relations for the height lower and higher than the turning point 0.6 h_i/H, respectively, and fitted the data, as shown in Figure 9, by regression with an approximately straight line (the dotted line in Figure 9) as the functional relationship curve of the distribution coefficient along the wall height ratio. At the same height, the difference in the distribution coefficient between different slope inclinations decreases with an increase in slope inclination. Consequently, a correlation formula is proposed to calculate the distribution coefficient with consideration on balance between the strict risk level and the straightforward mathematical expression. The correlation formula is shown in Exp. (1), in which ε denotes the slope of the retaining wall-back face with respect to the vertical direction in the radian value.

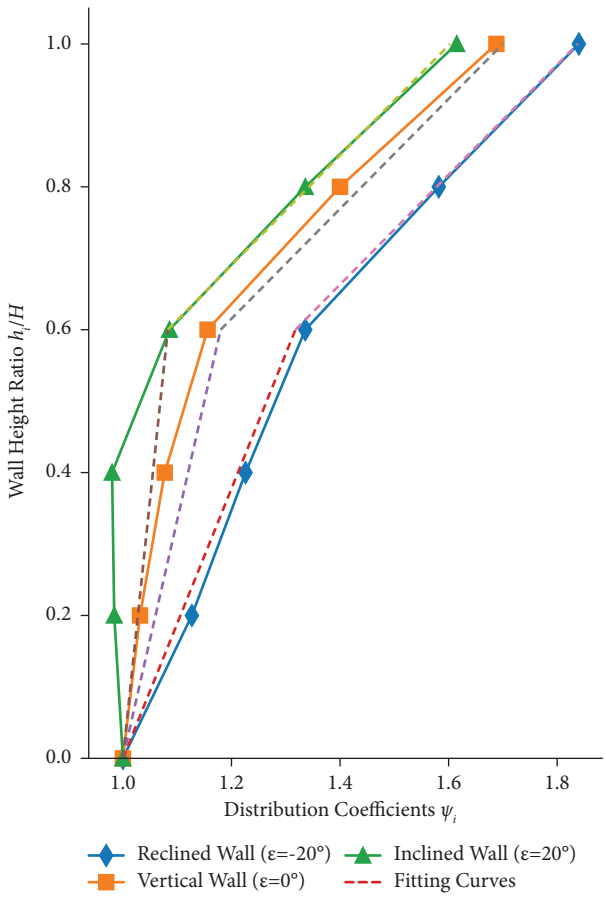

Figure 9: Fitting curves of the distribution coefficient ψ_i.

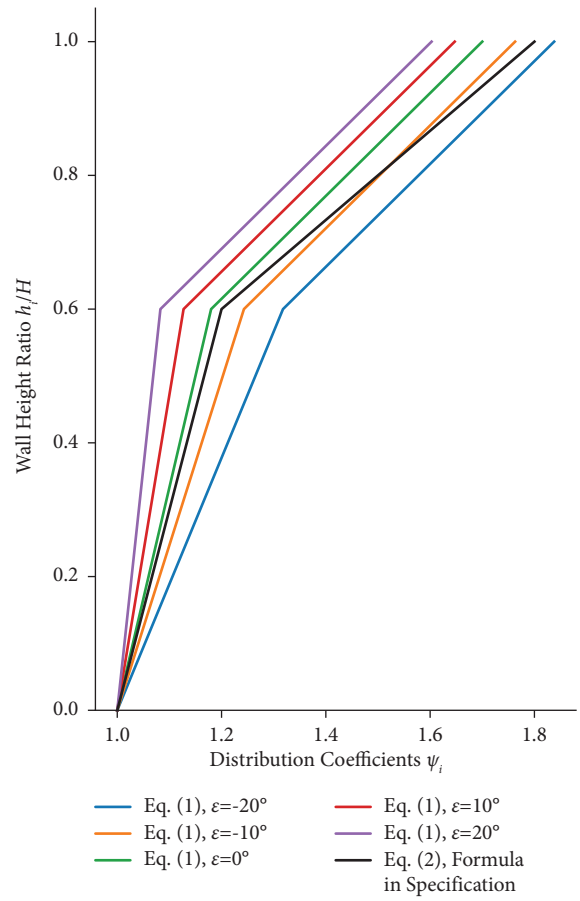

Figure 10: Comparison curve of results of Exp. (2) and Exp. (1).

$$\psi_i = \begin{cases} (0.55e^{-\varepsilon} - 0.25)\left(\dfrac{h_i}{H}\right) + 1.0, & 0 \le h_i \le 0.6H, \\ 1.3\left(\dfrac{h_i}{H}\right) + 0.33e^{-\varepsilon} + 0.07, & 0.6H < h_i \le H, \end{cases} \quad (1)$$

3.4. Comparison with the Current ψ_i Expression in the Specification. As discussed previously, the amplification effect of horizontal inertial loading on the wall itself along wall height shall be considered for the dynamic design of retaining walls. The design for ψ_i is dictated by the Chinese Specification of Seismic Design for Highway Engineering (JTG B02-2013). Its design expression for ψ_i is shown in the following expression [11]:

$$\psi_i = \begin{cases} \dfrac{1}{3}\dfrac{h_i}{H} + 1.0, & 0 \le h_i \le 0.6H, \\ \dfrac{3}{2}\dfrac{h_i}{H} + 0.3, & 0.6H < h_i \le H. \end{cases} \quad (2)$$

Figure 10 shows the comparison between the calculated distribution coefficient curve obtained by the proposed expression in this work (Exp. (1)) and that obtained from the specification (Exp. (2)). It can be seen that below 0.6 h_i/H, the results calculated by the specification formula are much similar to those of the vertical type but less than those obtained by the reclined type and greater than those obtained by the inclined type, respectively. Beyond 0.6 h_i/H, the specification results increased slower than the calculated ones by Exp. (1) and approached the results of the reclined wall of $\varepsilon = 20$. Nevertheless, the calculated data are roughly around the data calculated by Exp. (2), indicating the adaptability of proposed Exp. (1) in the retaining wall design. On the other hand, since the current specification does not consider the influence of wall-back inclination, the reclined retaining wall might be necessary to calculate the extra inertial load to improve the safety of the design, while the inclined retaining wall may not be needed to calculate the large inertial load.

In addition to the aforementioned typical wall inclination angles, we also calculated the distribution coefficients for other inclination angles. Figure 11 shows the change in the distribution coefficient versus wall-back inclination. It can be seen that wall-back inclination has an obvious influence on the distribution coefficient. At a specific wall height, the distribution coefficient steadily decreases with an increase in wall-back inclination. As Exp. (1) includes the influence of wall-back inclination, it might actually reflect the real response and might also be regarded as a more comprehensive relationship for retaining wall design.

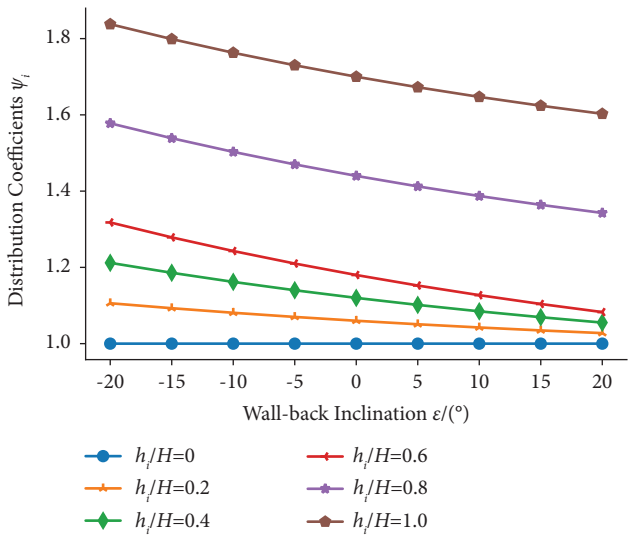

Figure 11: Relationship curve between the distribution coefficient and the wall-back inclination angle.

In addition, even though Exp. (1) is based on the results of the reclined, vertical, and inclined retaining walls, it might still be applicable to other forms of gravity-retaining walls, such as convex polygonal lines and stepped retaining walls, to calculate the distribution coefficient of horizontal seismic loading along wall height, as those walls can be reasonably simplified to reclined or inclined retaining walls via a geometry similarity rule for sections.

4. Conclusions

This paper experimentally examined the influence of the wall-back slope of retaining walls on the dynamic response to seismic waves on a shaking table test system. The inclination angles of the wall back have a significant effect on the seismic dynamic response of the retaining wall. The intensity of the seismic dynamic response increases with a decrease in wall-back inclination angles; the order of the degree of the seismic dynamic response is the reclined retaining wall > the vertical retaining wall > the inclined retaining wall. By adopting a risk security level of 90% probability, a calculation formula for the distribution coefficient of horizontal seismic action along wall height was proposed, in which the effect of the wall-back inclination angle was considered. Compared with the previous calculation formula involving no inclination angle, this improved one would better reflect the influence of retaining wall-back inclination on gravity-retaining walls and provide some guidance for the seismic design of gravity-retaining walls with different wall-back inclinations.

Data Availability

The data used to support the findings of this study are available from the corresponding author upon request.

Conflicts of Interest

The authors declare that they have no conflicts of interest.

Acknowledgments

This work was supported by the Special Knowledge Innovation Project of the Wuhan Science and Technology Bureau (Grant No. 2022010801010205) and the National Natural Science Foundation of China (Grant No. 41672309).

References

[1] H. Hu, Yu Huang, L. Zhao, and M. Xiong, "Shaking table tests on slope reinforced by anchored piles under random earthquake ground motions," *Acta Geotechnica*, vol. 17, no. 9, pp. 4113–4130, 2022.

[2] L. Tong, S. Ma, Q. Feng, D. Cui, and X. Ren, *Soil Mechanics*, China University of Geosciences Press, Wuhan, China, 2021, (In Chinese).

[3] X. Liu, S. Ma, H. Jia, T. Wu, Z. Hu, and Z. Zhu, "Numerical simulation of soil pressure characteristics of gravity retaining walls during earthquake," *Chinese Journal of Earthquake Engineering*, vol. 39, no. 4, pp. 750–758, 2017, (In Chinese).

[4] H. Gao, Z. Ji, Q. Xu, X. Zhang, Z. Wang, and C. Wang, "Seismic design method of retaining wall filled with EPS lightweight soil based on direct displacement," *Earthquake Engineering and Engineering Dynamics*, vol. 41, no. 5, pp. 13–21, 2021, (In Chinese).

[5] C.-C. Huang, S. –H. Wu, and H.-J. Wu, "Seismic displacement criterion for soil retaining walls based on soil strength mobilization," *Journal of Geotechnical and Geoenvironmental Engineering*, vol. 135, no. 1, pp. 74–83, 2009.

[6] Ministry of Transport of the People's Republic of China, *Specification of Seismic Design for Highway Engineering (JTJ 004-89)*, China Communications Press, Beijing, China, 1989, (In Chinese).

[7] X. Chen, *Two Improvements in Seismic Analysis of Retaining Structures*, Institute of Engineering Mechanics China Seismological Bureau, Harbin, China, 2003, (In Chinese).

[8] X. Zhou, *Distribution of Lateral Earthquake Load along Retaining wall Height*, Harbin Institute of Technology, Harbin, China, 2005, (In Chinese).

[9] N. Xu, *Restudy on Distribution of Lateral Earthquake Action along Height of Balance Weight Retaining wall*, Harbin Institute of Technology, Harbin, China, 2006, (In Chinese).

[10] C. Li, S. He, and W. Bao, "Research on height distribution coefficients of earthquake inertia forces on retaining structures," *Journal of Highway and Transportation Research and Development*, vol. 26, no. 1, pp. 51–56, 2009, (In Chinese).

[11] Ministry of Transport of the People's Republic of China, *Specification of Seismic Design for Highway Engineering (JTG B02-2013)*, China Communications Press, Beijing, China, 2013, (In Chinese).

[12] P. Nandakumaran, *Behavior of Retaining wall under Dynamic Loads*, Institute of technology roorkee, Chennai, India, 1973.

[13] C. S. Lai, *Behavior of Retaining wall under Seismic loading*, Department of Civil Engineenng, New Zealand, Oceania, 1979.

[14] C. Ren, *Study on Distribution Coefficient of Horizontal Seismic Stress along Gravity Retaining Wall*, China University of Geosciences, Wuhan, China, 2016, (In Chinese).

[15] J. Koseki, F. Tatsuoka, K. Watanabe, M. Tateyama, and K. Kojima, "Model tests of seismic stability of several types of soil retaining walls proc int workshop on seismic performance of geosynthetic-reinforced soil structures," *Reinforced Soil Engineering*, pp. 308–349, Advances in Research and Practice, New York, NY, USA, Marcel Dekker, 2003.

[16] D. Yang, L. Yao, and L. Jiang, "Experimental study of seismic earth pressure of GRW on soil site[J]," *Journal of disaster prevention and reduction*, vol. 27, no. 1, pp. 8–16, 2011.
[17] F. Jiao, L. Yao, L. Jiang, and J. Zhao, "Shaking table model experimental study on seismic soil pressure of GRW on rock site," *Journal of disaster prevention and reduction*, vol. 31, no. 3, pp. 316–322, 2011, (In Chinese).
[18] S. Nakajima, T. Ozaki, and T. Sanagawa, "1 g Shaking table model tests on seismic active earth pressure acting on retaining wall with cohesive backfill soil," *Soils and Foundations*, vol. 61, no. 5, pp. 1251–1272, 2021.
[19] H. Nakazawa, I. Tomohiro, D. Toru, O. Yasuhiro, S. Daisuke, and T. Hara, "Model tests on the stability of retaining walls with gabions under earthquake and rainfall conditions," in *Lecture Notes in Civil Engineering*, pp. 56–67, Springer, New York, NY, USA, 2022.
[20] Z. Sun, L. Kong, Y. Wang, and Z. Zhou, "Study on seismic response characteristics of a micropile-reinforced filled slope behind a cantilever retaining wall," *Chinese Journal of Rock Mechanics and Engineering*, vol. 41, no. 10, pp. 2109–2123, 2022, (In Chinese).
[21] M. Futaki, N. Ogawa, M. Sato, T. Kumada, and S. Natsume, "Experiments about seismic performance of reinforced earth retaining wall," in *Proceedings of the 11th World Conference on Earthquake Engineering*, Elsevier Science, New York, NY, USA, June, 1996.
[22] M. M. El-Emam and R. J. Bathurst, "Experimental design, instrumentation and interpretation of reinforced soil wall response using a shaking table," *International Journal of Physical Modelling in Geotechnics*, vol. 4, no. 4, pp. 13–32, 2004.
[23] S. Liu, F. Jia, X. Chen, and L. Li, "Experimental study on seismic response of soilbags-built retaining wall," *Geotextiles and Geomembranes*, vol. 48, no. 5, pp. 603–613, 2020.
[24] L. Wang, G. Chen, and S. Chen, "Experimental study on seismic response of geogrid reinforced rigid retaining walls with saturated backfill sand," *Geotextiles and Geomembranes*, vol. 43, no. 1, pp. 35–45, 2015.
[25] Y. Wang and S. Shi, "Research on earthquake induced earth pressure," *Progress of Hehai Science and Technology*, vol. 11, no. 3, pp. 85–89, 1991, (In Chinese).
[26] Y. Bao, Y. Huang, and C. Zhu, "Effects of near-fault ground motions on dynamic response of slopes based on shaking table model tests," *Soil Dynamics and Earthquake Engineering*, vol. 149, Article ID 106869, 2021.
[27] H. Sun, F. J. Niu, K. J. Zhang, and X. R. Ge, "Seismic behaviors of soil slope in permafrost regions using a large-scale shaking table," *Landslides*, vol. 14, no. 4, pp. 1513–1520, 2017.
[28] S. Lai, "Similitude for shaking table tests on soil-structure fluid model in 1-g gravitational field," *Soils and Foundations*, vol. 29, no. 1, pp. 105–118, 1989.
[29] M. L. Lin and K. L. Wang, "Seismic slope behavior in a large-scale shaking table model test," *Engineering Geology*, vol. 86, no. 2-3, pp. 118–133, 2006.
[30] K. L. Wang and M. L. Lin, "Initiation and displacement of landslide induced by earthquake — a study of shaking table model slope test," *Engineering Geology*, vol. 122, no. 1-2, pp. 106–114, 2011.
[31] A. Athanasopoulos-Zekkos, K. Lamote, and G. A. Athanasopoulos, "Use of EPS geofoam compressible inclusions for reducing the earthquake effects on yielding earth retaining structures," *Soil Dynamics and Earthquake Engineering*, vol. 41, pp. 59–71, 2012.